Electronic Supplementary Material (ESI) for Nanoscale.
This journal is © The Royal Society of Chemistry 2019

Supporting Information

Defect-targeted Self-healing of Multiscale Damage in Polymers

Yang Yang, Lei Gao, Jiaye Xie, Yao Zhou, Jun Hu, Qi Li, and Jinliang He**

State Key Laboratory of Power System, Department of Electrical Engineering, Tsinghua University, Beijing 100084, China

*Corresponding authors.
E-mail address: Li, Q. (qili1020@tsinghua.edu.cn), He, J. (hejl@tsinghua.edu.cn).

This PDF file includes:

Section S1: Dynamic size of γ-Fe_2O_3@PEG and PMMA chains

Dynamic light scattering tests

Regarding solid sphere particles and most macromolecules, the radius of gyration R_g is close to its hydrodynamic radius R_h characterized by dynamic light scattering (DLS) method. For the consistency of size comparison, the hydrodynamic radius distributions of the γ-Fe_2O_3, γ-Fe_2O_3@PEG nanoparticles (Fig. S1a) and the PMMA polymer chains (Fig. S1b) in acetone (0.5 wt.% at 25 °C, which coincides with the unperturbed state of PMMA in Θ solution)[2] were characterized by DLS (Wyatt DynaPro NanoStar, USA) tests. The Gauss fitting curves indicated that the peak R_h of γ-Fe_2O_3 is 9.4 nm and increases to 22.8 nm after surface grafting. The R_h distribution of PMMA exhibits two peaks at 2.16 nm and 38.5 nm. It is believed that the larger one represents the size of whole polymer chains while the smaller one represents some oligomer component which is actually very low in weight (or volume) percentage. Previous research with PMMA in Θ solvent demonstrated that the ratio R_g/R_h is 1.16,[3] the R_g of PMMA can be estimated as 44.6 nm which is slightly smaller than the hydrodynamic diameter of γ-Fe_2O_3@PEG (45.6 nm).

Through summarizing the previously published researches, the R_g can be calculated according to the molecular weight:[4]

$$\left\langle R_g^2 \right\rangle^{1/2} = 0.0290 M_W^{1/2} \quad (\pm 2.5\%) \quad \text{(nm)} \tag{S1}$$

The estimated R_g from the M_n is 43 nm, which verifies the results of DLS tests. According to the Gaussian chain model of linear polymer,[5] the relationship between the radius of gyration R_g and root-mean-square end-to-end distance R_e can be derived as:

$$\left\langle R_g^2 \right\rangle = \frac{1}{6} N b^2 = \frac{1}{6} \left\langle R_e^2 \right\rangle \tag{S2}$$

where N is the number of chain segments and b is the length of chain segment or Kuhn length. Then the R_e can be estimated around 100 nm which is used as the unit of length in the coarse-grained molecular simulation works.

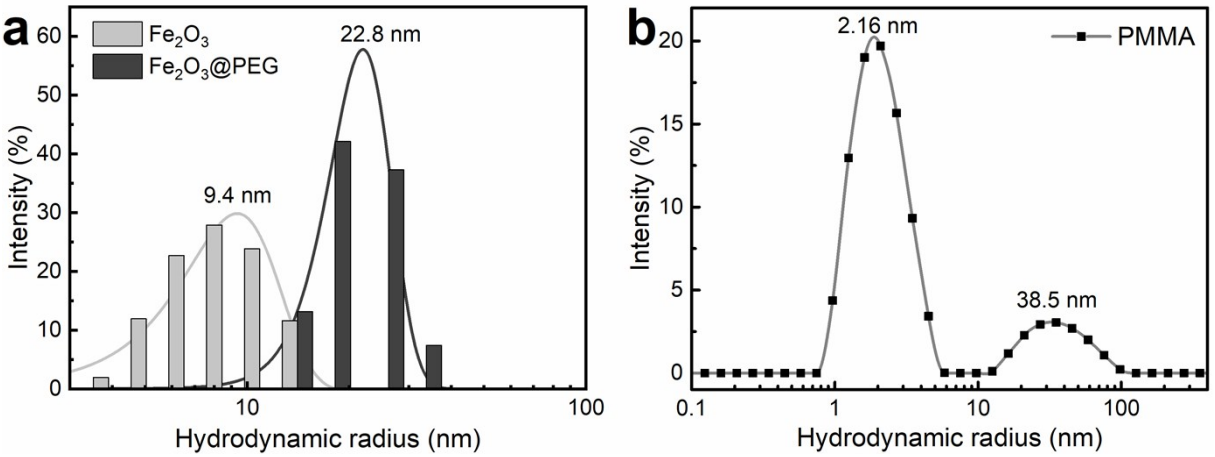

Fig. S1. Hydrodynamic radius distributions by DLS. (a) γ-Fe_2O_3, γ-Fe_2O_3@PEG and (b) PMMA tested in acetone at 25 °C.

Section S2: Mechanical fracture tests

The fracture tests were performed by displacement-controlled process (10 μm/s) on the tapered double cantilever beams (TDCB) specimen shown in Fig. S2.

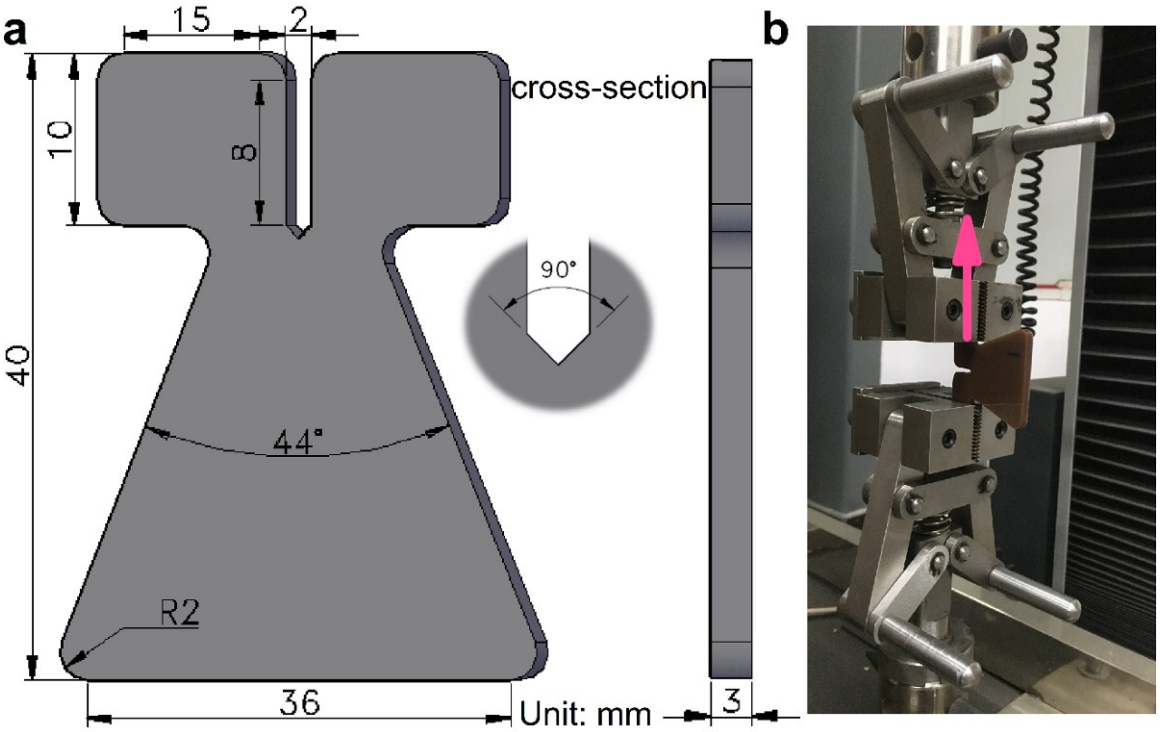

Fig. S2. Schematics of (a) TDCB shape and (b) the displacement-controlled process.

Section S3: Temperature difference in localized heating

Sample temperature distribution during the healing cycle

A typical healing cycle is demonstrated in Fig. S3. The temperature distribution was monitored by high-resolution infrared thermal imaging (IRTI). The heating was largely localized to the damaged region while the tested temperature difference is far below the real value for the limited spatial resolution of infrared camera.

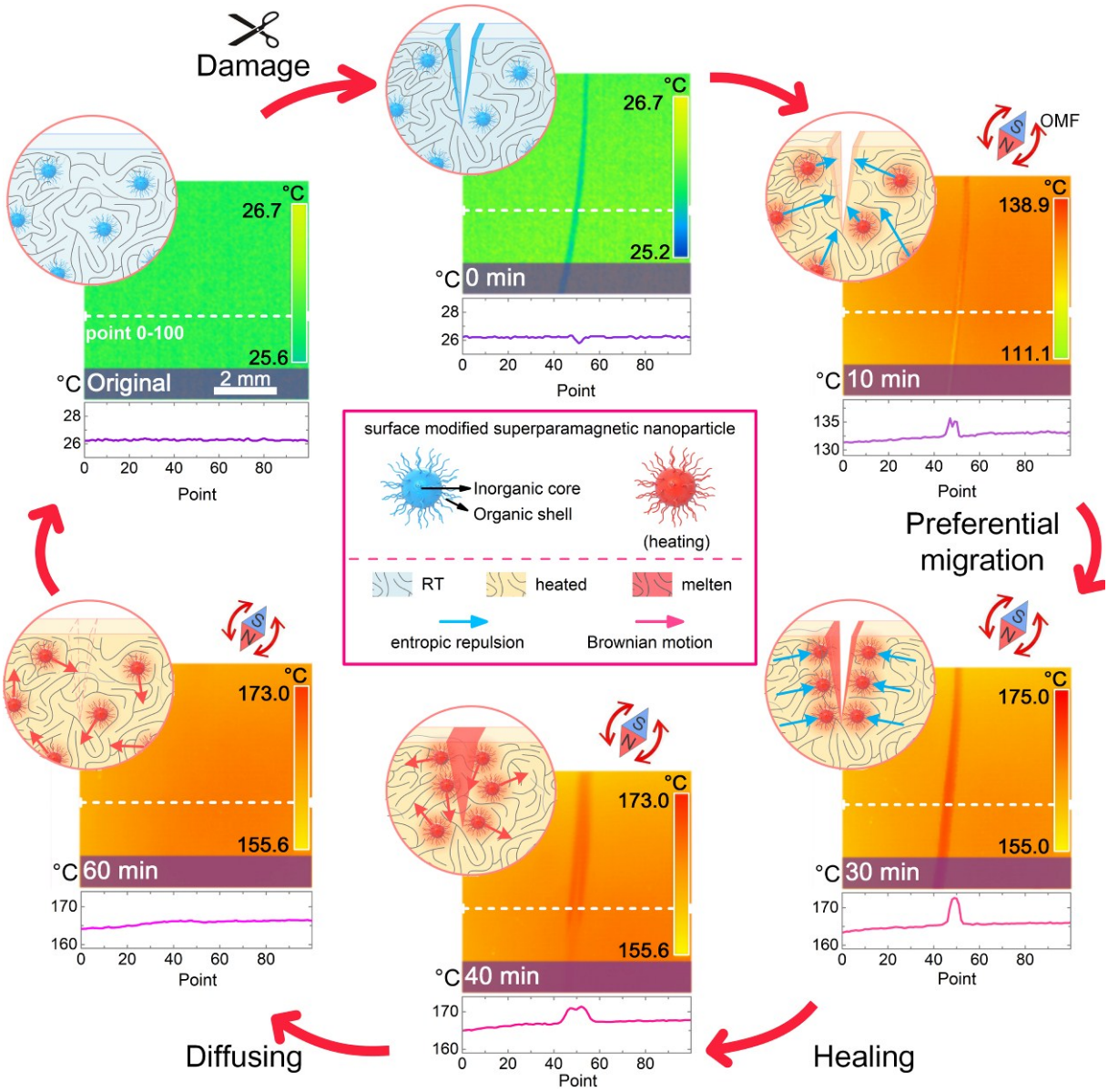

Fig. S3. Fundamental principles and characterization of the HMD. The IRTI images of the fractured 0.23 vol.% PMMA/γ-Fe_2O_3@PEG sample under magnetic field.

Finite element modeling (FEM) and simulation of localized heating

The detected temperature difference of defect region is highly underestimated by the limited spatial resolution of IRTI technique because the target size of high concentration band (about 1 μm, by TEM images in Fig. 1) is much smaller than the minimum pixel size of IR images (about 70×70 μm, Fluke TiX640 with micro lens), which is one of the most advanced infrared camera series. The detected temperature difference should be far below the real value which can be estimated by FEM simulation. The FEM simulation was carried out according to our previous work[1] and the following settings are modified according to Fig. S4a:

1) The Dirichlet boundary (constant temperature) condition is applied to the surrounding surfaces to simulate the adjacent 165 °C pixels.
2) The surface emissivity of thermal radiation ε=0.9, thermal conductivity of PMMA k=0.19 W/(m·K) and thermal capacity C_P=1420 J/(kg·K).
3) The heating power of the defect region is determined by parameter scanning until the average temperature of the surface line L_o equals the detected temperature of the crack edge (i.e., 172 °C).

The temperature distribution of the surface line L_o and internal line L_i are shown in Fig. S4b. The highest temperature of the defect region inside the sample is 202.2 °C which indicate that the magnetic field treatment can produce high temperature difference of 37.2 °C across 1.5 mm length-scale. Even for the surface exposed to the ambient, the temperature difference is more than 20 °C across dozens of micrometers.

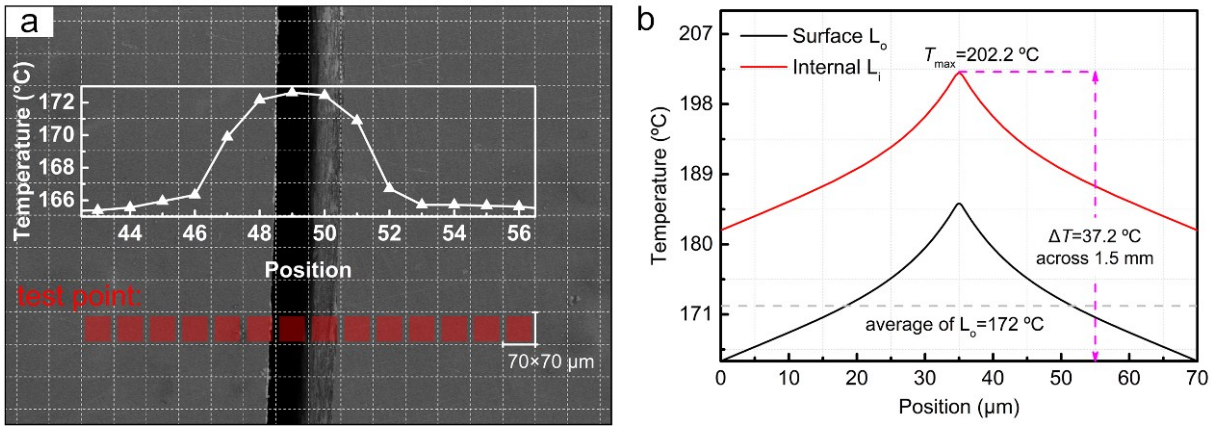

Fig. S4. Finite element modeling (FEM) and simulation of localized heating according to the method performed in our previous work.[1] (a) The pixel mesh and the temperature curve detected by IRTI (Fig. 1, 30 min). The red dot represents the detected region of each data point. (b) The temperature distribution of the surface line L_o and internal line L_i of the sample. The calculated temperature difference is 37.2 °C across 1.5 mm.

Estimation of local temperature for healing

To estimate the local temperature of defect region during “healing” process, the fractured 0.23 vol.% PMMA/γ-Fe_2O_3@PEG samples were annealed in air dry oven at various temperature for 1 h. Then the healing efficiency of annealed samples were tested and shown in Fig. S5. As the annealing temperature increases to 193 °C the healing efficiency reaches 98% which is close to the value of 1 h magnetic field treatment. The local temperature of defect region under magnetic field treatment can be estimated as 193 °C and this value is conservative because:

1) The temperature of the sample in oven rises to the set point within short time considering the high temperature atmosphere, the isothermal annealing time is nearly 1 h. The localized heating process of the samples treated under magnetic field is no more than 30 min (see Fig. S3). The healing efficiency actually reaches nearly 100 % after 30 min of magnetic field treatment (Section S4).
2) For the annealing treatment in oven, the sample temperature is homogeneous and it is fully melted at high temperature. For the magnetic field treatment, only the defect region is molten and higher fluidity (or local temperature) is needed to reach the same healing efficiency.

The pictures of the samples hung in the oven during annealing treatment indicate that the nanocomposite is soften above 180 °C and molten near 190 °C. Annealing treatment at 160 °C, which is close to the temperature of undamaged region under magnetic field treatment, maintains the dimensional stability of the sample. The localized heating brings high temperature difference which can heal the defect region without softening the whole material.

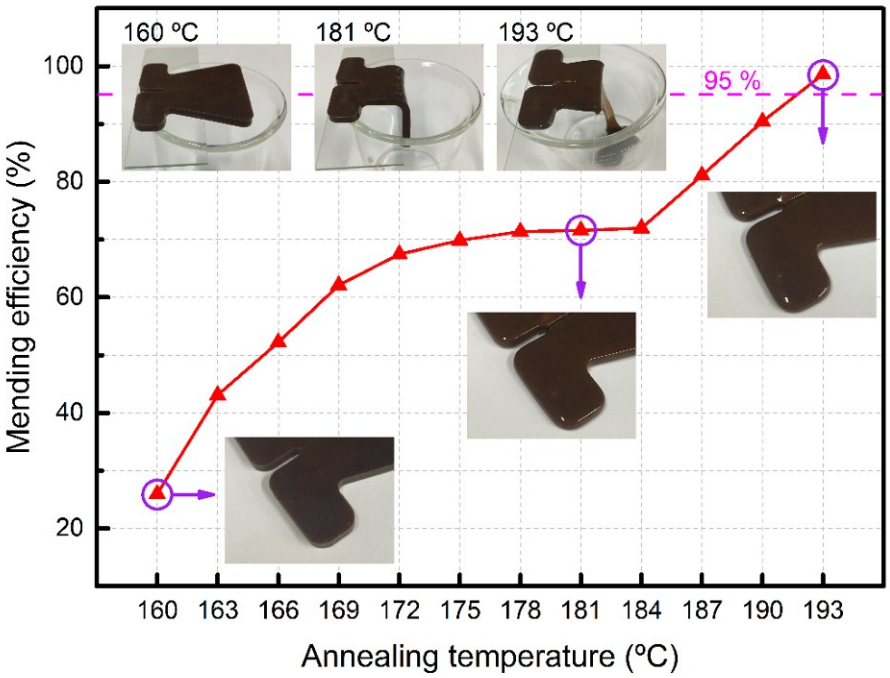

Fig. S5. Healing efficiency of PMMA/γ-Fe_2O_3@PEG after annealing treatment at different temperature in air dry oven for 1 h. To achieve the high healing efficiency by 1 h magnetic field treatment (above 95 %), the conservatively estimated temperature is at least 193 °C. Considering that the detected temperature of undamaged region in Fig. 1 (30 min) is 163 °C, the temperature difference produced by localized heating under magnetic field should be larger than 30 °C.

Section S4: MFM characterization of bare γ-Fe_2O_3 nanoparticles

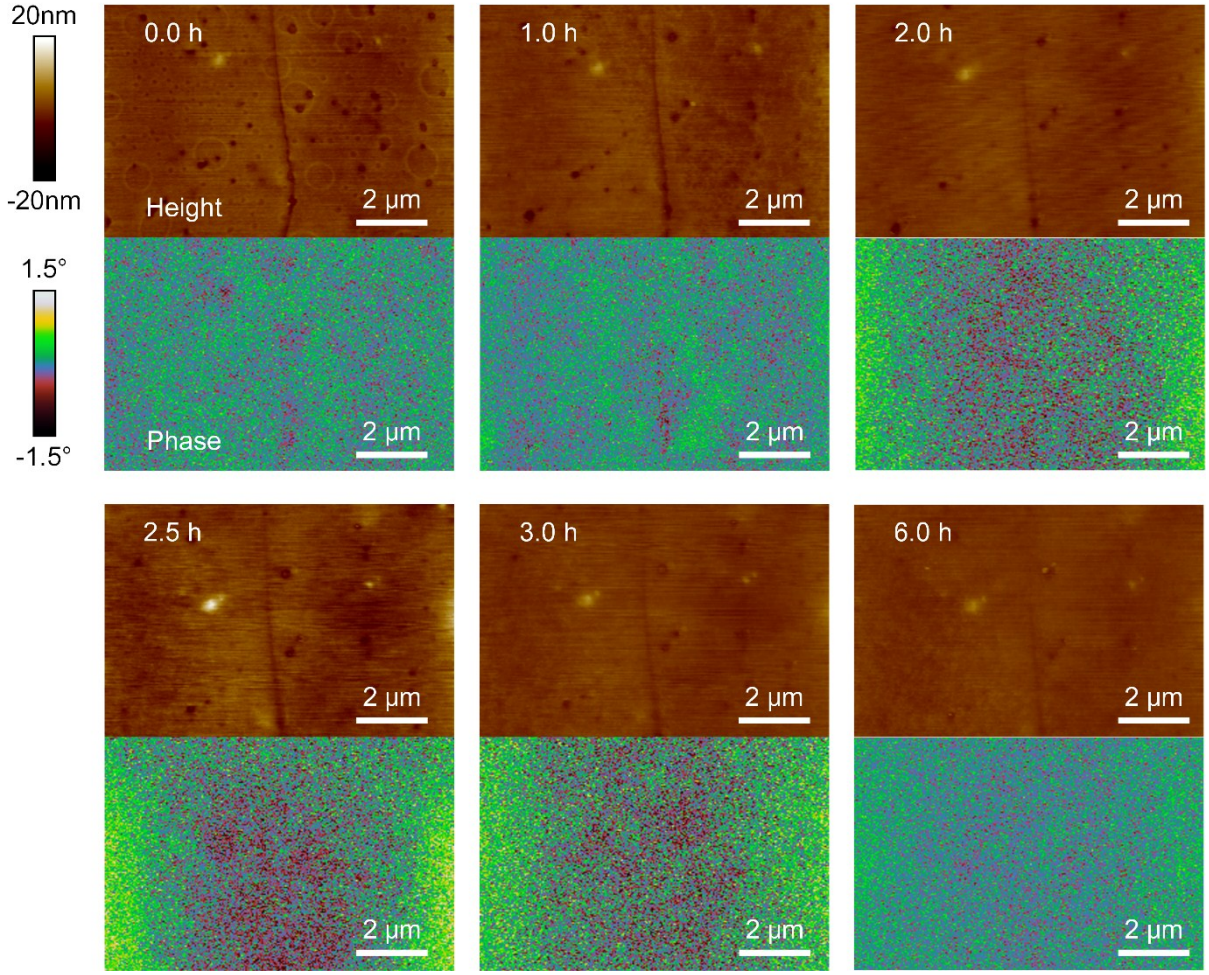

Fig. S6. MFM tests of 0.23 vol.% PMMA/γ-Fe_2O_3 nanocomposite film. Topology (height) and magnetic phase images (10×10 μm) of the spin coated films near the cracks after different periods of annealing treatment at 120 °C (see Methods section).

Section S5: Restoration of mechanical properties in PMMA nanocomposites

Pristine load-displacement curves of the TDCB samples

The load-displacement curves of the PMMA and PMMA/γ-Fe_2O_3@PEG nanocomposite TDCB specimens are shown in Fig. S7. The stretching is stopped immediately after cracking so that the fracture load can be recorded without snapping the TDCB sample.

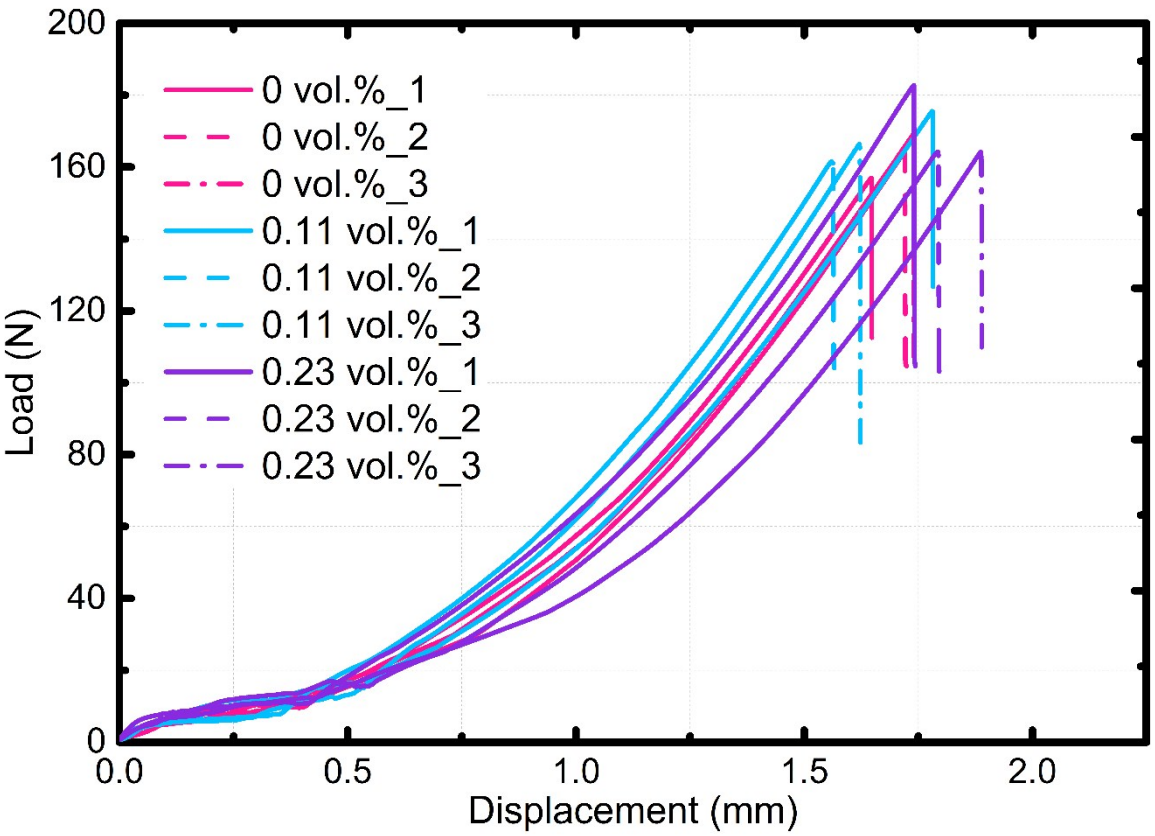

Fig. S7. Load-displacement curves of the TDCB specimens. The PMMA and PMMA/γ-Fe_2O_3@PEG (containing 0 vol.%, 0.11 vol.% and 0.23 vol.% nanoparticles) TDCB specimens were tested with 3 parallel samples by the displacement controlled process until fracture.

Healing efficiency of micro-scale damaged TDCB specimens

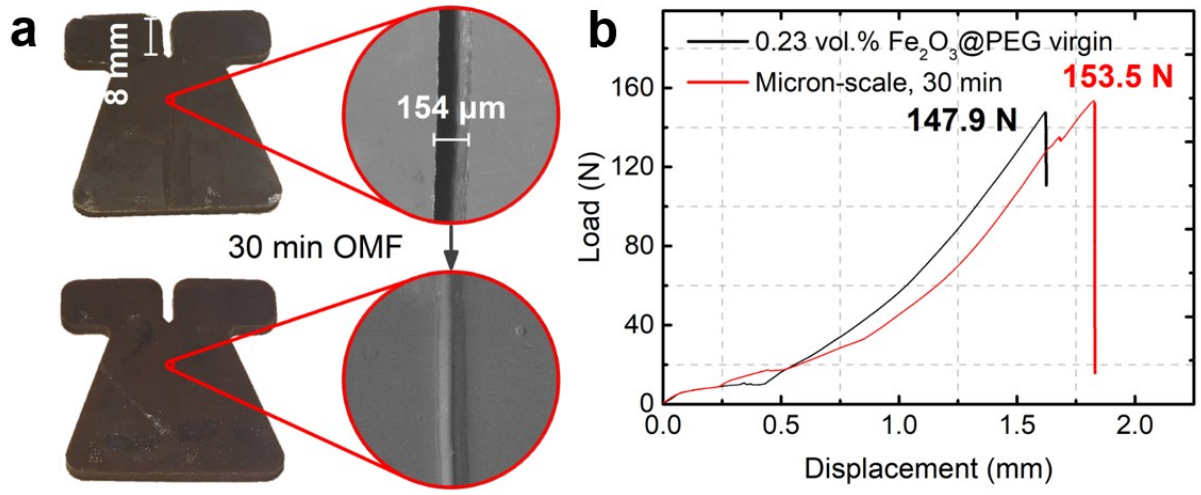

Fig. S8. Mechanical restoration of the 0.23 vol.% nanocomposite with micrometer-scale damage. (a) Optical and local SEM images of the crack region. (b) Load-displacement curves of virgin and 30-min magnetic field healed sample.

The magnetic mending efficiency of the micron-scale fractured 0.23 vol.% PMMA/γ-Fe_2O_3 nanocomposites with different time of magnetic heating are shown in Fig. S9. After 15- and 30-min treatment under the same OMF, the PMMA/γ-Fe_2O_3 samples exhibit only 35.2% and 55.7% recovery of the fracture load which is close to the healing efficiency of homogeneous heating treatment at 165 °C (Fig. S5). Without the steric repulsion provided by surface modification, the bare nanoparticles cannot migrate towards the crack nor generate localized heating to heal. For the heating time shorter than a standard healing cycle (e.g. 60 min for healing of microscale crack as shown in Fig. S3), the healing efficiency increases with the increasing of heating time.

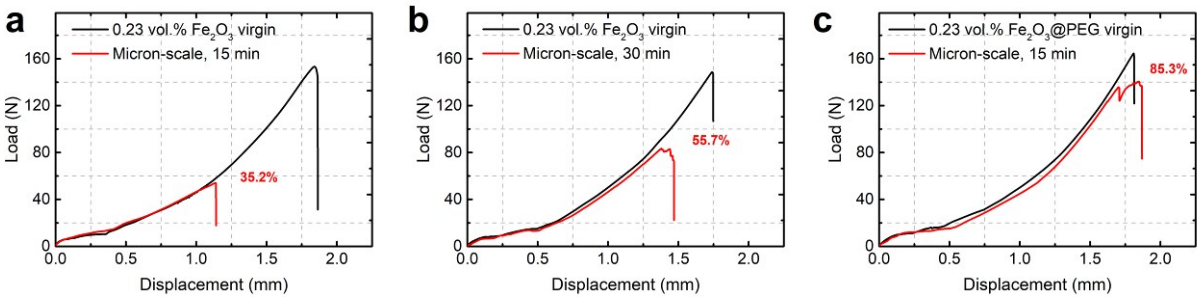

Fig. S9. Mending efficiency of 0.23 vol.% PMMA/γ-Fe_2O_3 and PMMA/γ-Fe_2O_3@PEG after different time of OMF treatment. Virgin and re-cracking load-displacement curves of the micron-scale damaged (a, b) PMMA/γ-Fe_2O_3 and (c) PMMA/γ-Fe_2O_3@PEG TDCB specimens after 15 min and 30 min of mag magnetic mending under OMF.

Table S1. Statistical mechanical mending efficiency of the samples.

Sample	0.11 vol.% γ-Fe_2O_3	0.23 vol.% γ-Fe_2O_3	0.11 vol.% γ-Fe_2O_3@PEG	0.23 vol.% γ-Fe_2O_3@PEG
15 min OMF	Not mended	44.2 ± 8.9 %	30.7 ±6.7 %	84.7 ± 4.5 %
30 min OMF	37.3 ± 4.3 %	53.0 ± 2.7 %	71.1 ± 5.3 %	102.1 ± 2.8 %

Section S6: Electrical conductivity test of PFSA/γ-Fe_2O_3@PEG

The 0.38 vol.% PFSA/γ-Fe_2O_3@PEG samples were prepared by solution mixing then casted in a 8×14 mm sample cell, both sides were pasted with conductive rubber as the electrodes of the polymer sample (Fig. S10). Conductivity tests of the sample were performed under 5, 10, 15, 20 V (0.625, 1.25, 1.875, 2.5 V/mm) at 30 °C. After the voltage was applied for 10 min, the polarization process tends to be stable and the final current is recorded to calculate electrical conductivity. Considering the proton-conducting mechanisms of the PFSA membrane, the magnetic healing process would influence the moisture content and the conductivity of the sample. Before the conductivity measurement, the samples were first conditioned in deionized water at room temperature for 30 min then dried at 60 °C for 4 h. The electrical conductivity of pure PFSA and PFSA/γ-Fe_2O_3@PEG samples are shown in Table S1. By soaking the sample cell into liquid nitrogen, the cracks can be generated due to the differences in the thermal expansion coefficients of the film and sample cell.

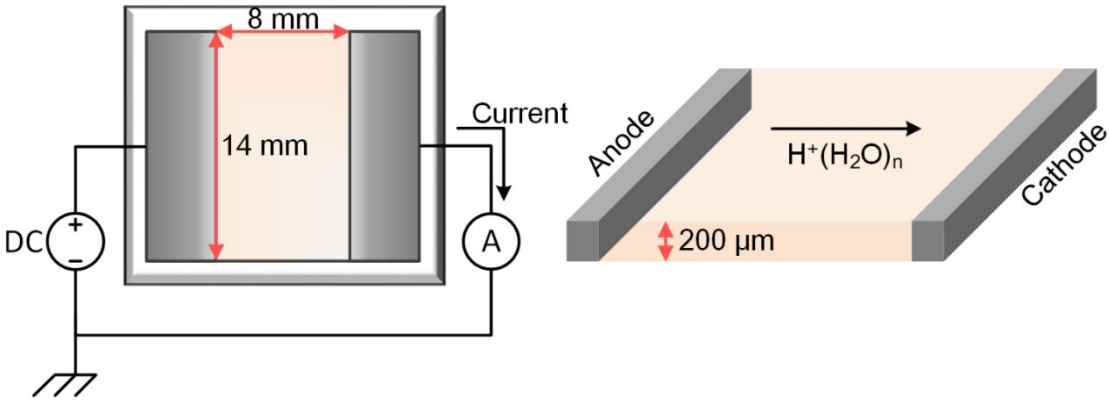

Fig. S10. Schematic diagram of the conductivity tests and the structure of the PFSA/γ-Fe_2O_3@PEG sample.

Table S2. Electrical conductivity of PFSA and PFSA/γ-Fe_2O_3@PEG under different electrical fields (unit: S/m).

Electrical field	2.5 V/mm	1.875 V/mm	1.25 V/mm	0.625 V/mm
PFSA	0.01578	0.01537	0.01284	0.00837
PFSA/γ-Fe_2O_3@PEG	0.01581	0.01106	0.01168	0.00560

Section S7: Glass transition temperature of PMMA

Differential Scanning Calorimetry (DSC, TA Q500, USA) tests were carried out at the heating rate of 15 °C /min (close to the heating rate of magnetic heating). The PMMA and 0.23 vol.% PMMA/γ-Fe_2O_3@PEG nanocomposite samples were first heated above the glass transition temperature (T_g) to remove thermal history then tested again. The second heating curve is shown in Fig. S11 and the T_g can be estimated as about 109 °C. Nano doping of 0.23 vol.% γ-Fe_2O_3@PEG has negligible impact on the glass transition temperature of PMMA.

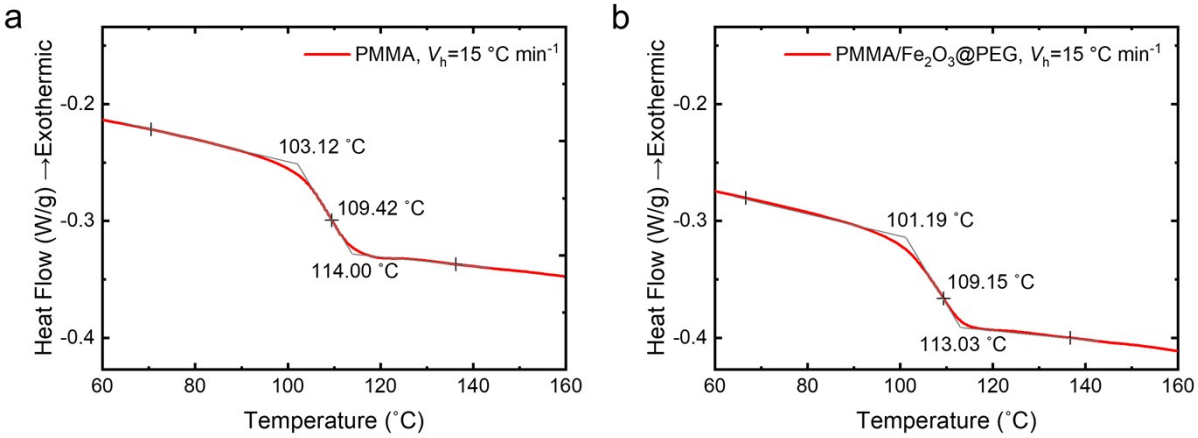

Fig. S11. DSC tests of the (a) PMMA matrix and (b) 0.23 vol.% PMMA/γ-Fe_2O_3@PEG nanocomposite samples. The heating curves show that the glass transition temperature of PMMA is about 109 ºC.

Supplementary References

(1) Y. Yang, *et al.*, Self-healing of electrical damage in polymers using superparamagnetic nanoparticles, *Nat. Nanotech.*, 2019, **14**, 151.

(2) T. Arai, N. Sawatari, T. Yoshizaki, Y. Einaga and H. Yamakawa, Excluded-volume effects on the hydrodynamic radius of atactic and isotactic oligo- and poly(methyl methacrylate)s in dilute solution, *Macromolecules*, 1996, **29**, 2309-2314.

(3) H. U. ter Meer, W. Burchard and W. Wunderlich, Quasi-elastic light scattering from polymethylmethacrylate in a good and a theta solvent, *Colloid Polym. Sci.*, 1980, **258**, 675-684.

(4) M. Schmidt and W. Burchard, Translational diffusion and hydrodynamic radius of unperturbed flexible chains, *Macromolecules*, 1981, **14**, 210-211.

(5) M. Doi and S. F. Edwards, The theory of polymer dynamics, *Oxford University Press*, New York, USA 1988.